EVALUATION OF FIBRE LENGTH DISTRIBUTION IN A SHORT GLASS FIBRE REINFORCED PA-6

Camilla Ravalico[1,*], Francesca Cosmi[1]

[1] Department of Engineering and Architecture, University of Trieste, Via A. Valerio 10, 34127 Trieste, Italy

[*]corresponding author: e-mail: cosmi@units.it

Resume

The aim of this work is to evaluate the fibre length distribution in a polyamide reinforced by short glass fibre. The fibre length and the fibre orientation distributions strongly influence the mechanical properties of short fibre reinforced composites. The sample investigated is a 30GFPA6 (polyamide-6 reinforced by 30 % by weight glass fibre), extracted from an injection-moulded plate. The digital reconstruction of the three-dimensional structure of the sample was obtained by synchrotron radiation micro-computed tomography (micro-CT), a high spatial resolution non-destructive technique. One global and one local method have been tested for the automatic evaluation of the fibre length distribution in our sample. The global method is based on the mean fibre length distribution computed from the Star Length Distribution (SLD), a morphological parameter. The local method is based on a 3D skeletonize function. The results are discussed in the light of the experimental data available in literature.

Article info

Article history:
Received 04 August 2015
Accepted 26 August 2015
Online 29 September 2015

Keywords:
Micro-CT;
Short glass fibre composites;
Polymer-matrix composites;
Fibre length distribution.

Available online: http://fstroj.uniza.sk/journal-mi/PDF/2015/16-2015.pdf

ISSN 1335-0803 (print version)
ISSN 1338-6174 (online version)

1. Introduction

Composite materials, like short fibre reinforced polymers, are widely employed. It is well known that the mechanical properties of short fibre reinforced polymers (SFRP) result from the combination of numerous factors, mainly matrix and fibre properties, fibre length distribution and fibre orientation distribution [1]. The morphological characteristics depend on the injection moulding process, the shape of the part, the thickness of the component and the type of injection gates [2].

Starting from the very simple rule of mixtures, several micro-mechanical models have been proposed to predict SFRP properties, which take into account the fibre geometry and the influence of fibre length on the shear strain distribution at the fibre end. The Cox or shear-lag model [3] assumes a linear elastic matrix, can be used to determine the SFRP Young's moduli and is based on the transfer of normal strain from matrix to fibre due to transversal strain on the interface. This model uses the fibre and the matrix Young's moduli, the fibre volumetric fraction, the fibre orientation, the mean fibre length and the fibre diameter. Many of these characteristics are known because they are typical for the material, others, like the mean fibre length, need to be determined experimentally. The Kelly-Tyson model [4] considers a rigid-plastic model of the matrix and introduces the concept of critical fibre length, that is the minimum fibre length that allows to obtain the maximum stress in the fibre, ensuring that failure is due to fibre rupture and enforcing an optimal use of reinforcement. Two different approaches are possible to model failure: one based on the mean fibre length, and

one based on the fibre length distribution. Bowyer and Bader modified the Kelly-Tyson method, introducing the fibre length distribution and the fibre orientation distribution into the model [5]. Fu and Lauke investigated the influence on the tensile strength of SFRP of the mean, most probable (mode) and critical fibre length, and of the fibre orientation distribution and coefficient [6]. In all models, both fibre orientation and fibre length distribution are fundamental to mechanical properties.

For the experimental analysis of the fibre orientation distribution in SFRPs, the optical observation of the fibre is widely used. The method is based on the observation of the elliptical footprints left by the fibres on sections of the sample. Starting from the footprint, the fibre orientation angles can be obtained [7]. The optical method needs to analyze each single fibre to obtain the fibre orientation distribution. Furthermore, this is a destructive method and the accuracy of the measurements depends on the quality of the obtained section planes [8]. However, its use is widespread, thanks to the relative simplicity of the required setup, particularly if compared with micro tomography. The micro Computed Tomography (micro-CT) is a non-destructive technique that consists in the acquisition of a large number of radiographic projections taken at different angular positions of the sample with respect to a source of X-ray. The projections are then processed using retro-projection algorithms for creating a digital reconstruction of the original sample. A 3D image of a SFRP sample, once reconstructed by micro-CT, can provide a detailed representation of the internal structure of the sample [9] that can be directly used in numerical models [10] or analyzed with morphological methods, for example those based on the Mean Intercept Length (MIL) concept [11 - 17]. Using the MIL approach it is possible to characterize the internal fibre structure by means of a second order fabric tensor. A fabric tensor is a directional quantity used to describe the directionality features of a complex microstructure, giving a compact representation of the anisotropy preferred orientations [18]. Experimental methods can be also used to verify the fibre orientation distribution predictions obtained by software simulating the injection moulding process [3, 19 - 21].

The fibre length distribution knowledge is fundamental for the implementation of the failure models and several methods exist to analyze it. The most common one is the optical method, a destructive technique that consists in a physical separation of the fibre from the matrix by hydrolysis or burning and in the observation at the microscope. This method is very easy to implement in term of the required setup. On the other hand, the operation is at risk of breaking various fibres during the extraction, due to fibre-polymer interaction, fibre-fibre interactions and fibre contact with surfaces of processing equipment [22, 23].

On the other side, the partially non-destructive technique based on the micro-CT used in this project is suitable for the analysis of the fibre length distribution as well as for the already discussed fibre orientation assessment.

Starting from the digital reconstruction of the sample, two different approaches were employed to obtain the fibre length in the examined sample: one global and one local. The global method uses the concept of Star Length Distribution (SLD) to determine the mean fibre length [24, 25]. The local method skeletonizes and evaluates each single fibre in the reconstruction. The results are compared with the experimental data available in literature.

2. Materials and methods

2.1 Materials

An ISO 527-2 [26] standard specimen obtained from an injection moulded rectangular plate of short glass fibre (30 % by weight) reinforced polyamide 6, PA6-GF30, was analysed. The examined sample (4 × 12 × 3.2 mm) was

extracted from the specimen, and is highlighted in black in Fig.1.

The 3D reconstruction of the specimen was obtained by synchrotron radiation micro-computed tomography (micro-CT), a technique that combines the advantages of a non-destructive technique with a high spatial resolution. The tomographic scans were obtained at YRMEP beamline of Elettra (Trieste, Italy), working with an energy of 20 keV. The micro-CT consists of the acquisition of a large number of radiographic projections taken at different angular positions of the sample. The sample is placed on a rotary table that allows it to rotate with respect to the source of X-ray, completing 180° of rotation. From the different angular projections obtained, using specific algorithms, it is possible to reconstruct the slices that represent the transverse sections of the sample. By stacking the sequence of slices it is then possible to obtain a full 3D representation of the sample, and to visualize its internal structure in 3D.

The results were 8-bit images that have gray tones between 0 and 255. The Volume of Interest (VOI), 396×343×431 voxel (3.564×3.087×3.879 mm^3), 9 μm resolution, was extracted from the completely reconstructed volume.

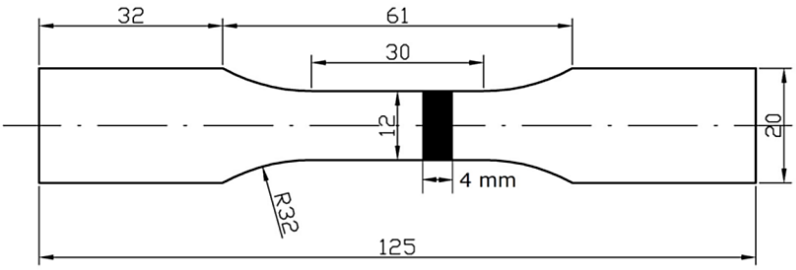

Fig. 1. ISO 527-2 standard specimen. The volume subjected to micro-CT is shown in black.

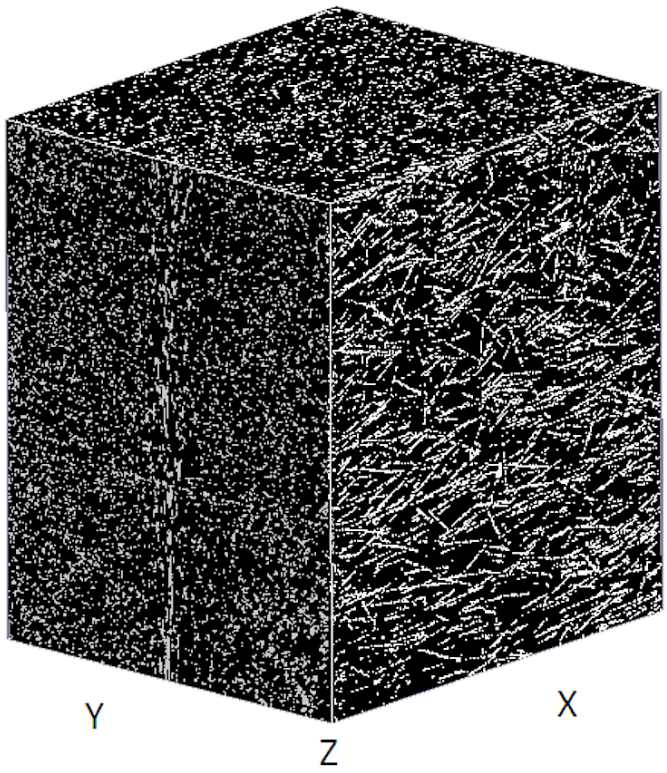

Fig. 2. 3D reconstruction of the VOI after the fibre segmentation.

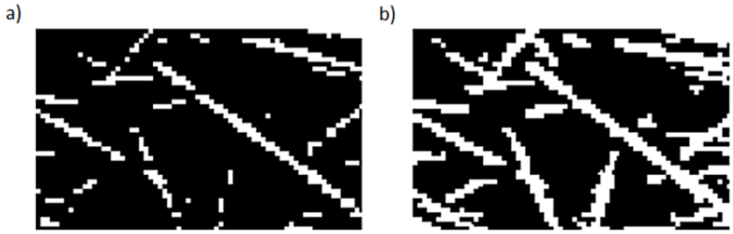

Fig. 3. a) Original image; b) Image after the enhance contrast function.

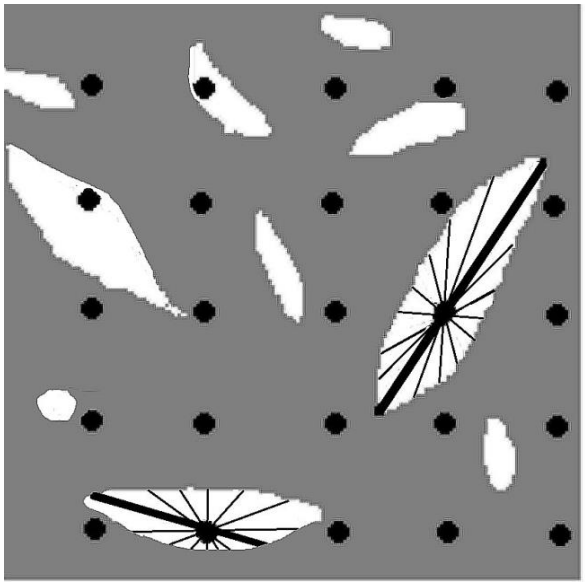

Fig. 4. Star length distribution (SLD) concept.

The 3D micro-CT reconstruction was segmented to identify fibre from matrix. The segmentation was a necessary step in order to univocally identify the different phases, in our case fibre and matrix. The chosen approach consists in setting the threshold value that allows to match known data with experimental ones, as proposed in [11]: since the glass fibre fraction charging the sample is known, because the manufacturing process imposed it, the fibre threshold can be obtained by requiring that the fibre volumetric fraction (FV/TV) in the reconstructed volume matches the physical fibre volumetric fraction.

In this work we used a sample with a fibre fraction equal to 30 % of the total weight, which corresponds to an ideal 15.92 % fibre volumetric fraction. The result of the segmented sample is shown in Fig. 2, where the fibres are shown in white.

The images were also pre-processed using the enhance contrast function in order to improve the definition of fibre, Fig. 3. The enhance contrast function introduced a neglectable change in the FV/TV, from 0.1553 to 0.1568.

2.2 Methods

Starting from the 3D sample reconstruction, two different approaches are presented in this paper: one global and one local.

2.2.1 Global method

Instead of trying to reconstruct exactly each single fibre, the global method uses the Star Length Distribution (SLD) concept. The SLD is a morphological parameter, generally used to evaluate some form of architectural anisotropy. Anisotropy is generally described by the main directions that are directed perpendicular to the planes of symmetry

in the structure, and by a number that describes the concentration of directions around the main directions. Fabric tensor provide an easy description of architectural anisotropy with a 3×3 matrix, where the eigenvectors give the main directions, and the eigenvalues represent the degree of concentration around the main directions [18]. The SLD procedure used is implemented in the Quant3D software, and computes the mean fibre length in a set of directions [27]. For a given structure composed by two different constituents (fibre and matrix in our case), the SLD was determined by placing a pattern of P points, and by measuring the length of the lines emanating from each point within the fibre in the different directions until they hit a boundary, as show in Fig. 4. It should be noted that the number p of valid points examined is always lower than P: in fact only the points situated on the fibre are considered valid for analysis.

In each valid point, the maximum fibre length s_j was evaluated. The SLD $l_i(\omega)$ is defined by equation (1) as the average of s_j in each direction ω [28].

$$l_i(\omega) = \frac{1\sum_{j=1}^{p} s_j(\omega)}{p} \quad (1)$$

where p is the number of examined valid points. We used P = 2000, and N = 513 different orientations.

It should be pointed out that the minimum measured length corresponds to the fibre diameter D_f.

The fibre length distribution can be described by the average fibre length (L) and by the weight average fibre length (L_w), which are expressed by equations (2) and (3):

$$L = \frac{\sum_{i=1}^{N} n_i l_i}{N} \quad (2)$$

$$L_w = \frac{\sum_{i=1}^{N} n_i l_i^2}{\sum_{i=1}^{N} n_i l_i} \quad (3)$$

where counting the different SLD having length l_i, n_i were found with l_i length.

2.2.2 Local method

The local method is based on the "Analyze skeleton" function, implemented in Fiji software. The method computes each fibre length [29, 30].

The "Skeleton" function takes each single fibre in the binary 3D images stack and erodes all the material until the fibres are reduced to single-pixel-wide shapes, alias the skeletons of the fibres, which can be assumed as lines. The algorithm, developed by Lee, Kashyap and Chu [31], calculates the index number for each object pixel, and uses the lookup table to decide if the pixel is eliminable: this process is repeated until no pixel can be eliminated. The "Analyze skeleton" function was then used to measure the 3D length of the skeleton of each fibre with a three-pass non-recursive approach [32].

The fibre length distribution, can be described also in this case by the average fibre length (L) and by the weight average fibre length (L_w), which are expressed by equations (4) and (5):

$$L = \frac{\sum_{i=1}^{N\prime} n\prime_i l\prime_i}{N\prime} \quad (4)|$$

$$L_w = \frac{\sum_{i=1}^{N\prime} n\prime_i l\prime_i^2}{\sum_{i=1}^{N\prime} n\prime_i l\prime_i} \quad (5)$$

where N' is the number of measured fibres and n'_i the numbers of fibres having length l'_i.

3. Results and discussion

Fig. 5 shows the polar plot of the SLD measurements in each of the 513 directions examined.

This polar diagram can be approximated by an ellipsoid or, equivalently, a second order tensor. The tensor eigenvectors and eigenvalues, representing the principal directions and axes of this ellipsoid, are shown in Table 1.

The fibre length distribution obtained with the global method is shown in Fig. 6.

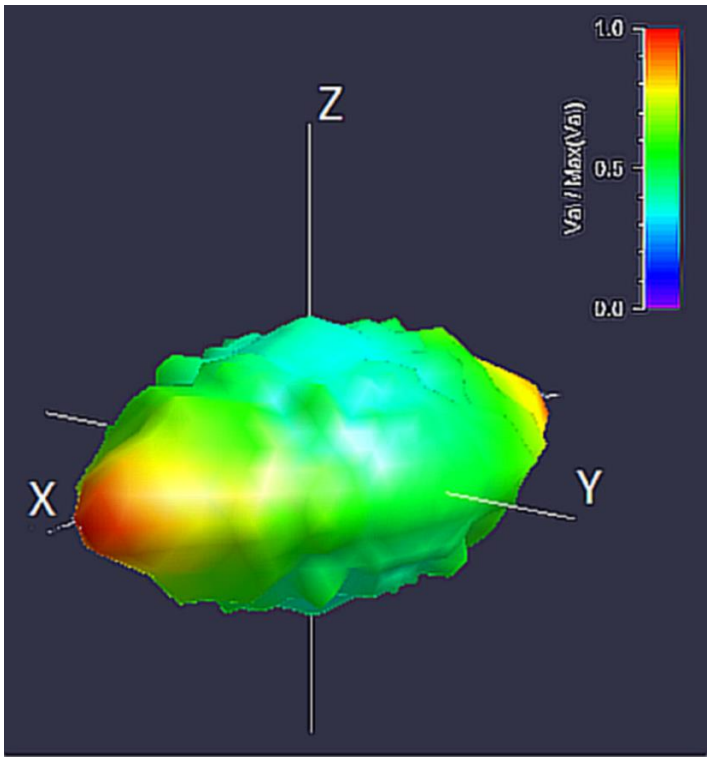

Fig. 5. Polar plot of the SLD measurements in each of the 513 directions examined.
(full colour version available online)

Table 1

Eigenvalues and eigenvectors from the SLD calculations

Eigenvalues	**Eigenvectors**		
0.469	-0.999	-0.019	0.014
0.299	-0.019	0.999	-0.006
0.232	-0.014	-0.006	-0.999

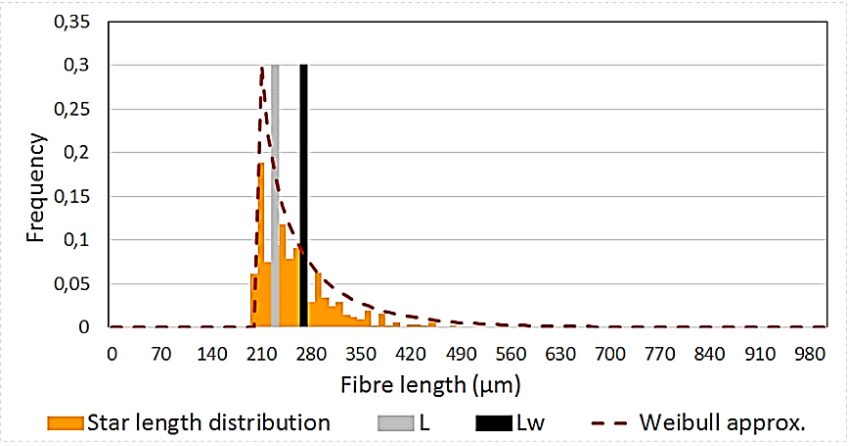

Fig. 6. Global method: fibre length distribution, L, L_w, Weibull approximation.
(full colour version available online)

The results of the local approach calculations are depicted in Fig. 7. It should be pointed out that the global method considers all the fibres, but does not show the shortest and the longest fibre lengths because it computes the average in each direction.

The results, summarized in Table 2, were in agreement with the experimental data available in literature for samples of PA6-GF30 and accessible in [1, 11].

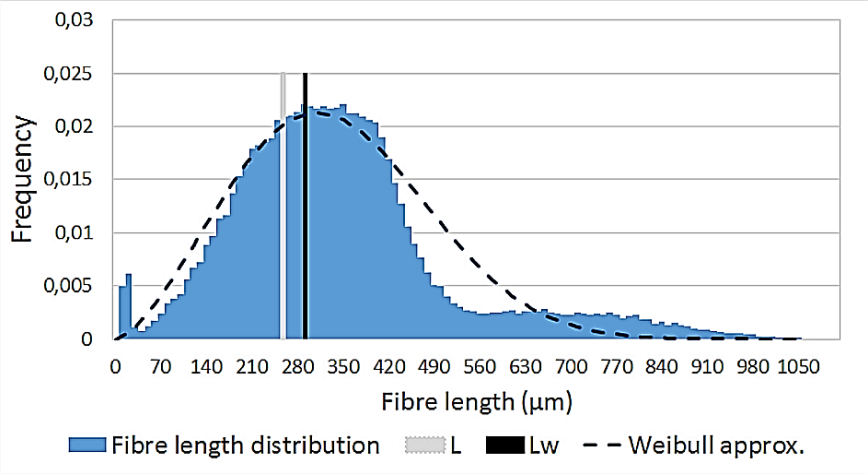

Fig. 7. Local method: fibre length distribution, L, L_w, Weibull approximation. (full colour version available online)

Table 2

Results of the fibre length distribution: L, L_w, D_f, obtained with the global method, the local method and experimentally.

	Global method	Local method	Experimental [1, 11]
L (µm)	234	256	200-300
L_w (µm)	275	262	275
D_f (µm)	10.2	-	10.5

4. Conclusion

The fibre length distribution in a sample of short fibre reinforced polyamide (PA6-GF30), extracted from an injection moulded plate, was evaluated and presented in this paper. The internal microstructure of the sample was reconstructed by micro-CT using synchrotron radiation and the fibre length distribution was successively computed with two different approaches: one global method, based on the Star Length Distribution (SLD) concept implemented in the Quant3D software, and a local method, based on the skeletonize function implemented in the Fiji software.

The analysis of the fibre length distribution is very important to characterize the short fibre reinforced composites behavior according to several models proposed in literature [3 - 6] and discussed in the Introduction section. The results obtained with both automatic approaches were in agreement with the data available in literature for samples of the same material and obtained experimentally with a destructive method.

In the future, our approach will be further validated by analyzing a larger number of samples having different fibre charges. Moreover, these results will be compared with those obtained with commercial software.

Acknowledgement

The authors would like to thank Prof. A. Bernasconi, Politecnico di Milano, who provided the sample examined in this study. The authors would also like to thank Diego Dreossi, SYRMEP beamline, Elettra (Trieste, Italy), for his assistance during the micro-CT acquisitions.

References

[1] A. Bernasconi, P. Davoli, A. Basile, A. Filippi: Int. J. Fatigue. 29(2) (2007) 199-208.

[2] J. L. Thomason: Compos. Sci. Technol. 59(16) (1999) 2297-2422.

[3] P.A. Erikson, A.C. Albertsson, P. Boydel, G. Parutzsch, J.A.E. Manson: Polym. Compos. 17(6) (1996) 830-839.

[4] A. Kelly, W.R. Tyson: J. Mech. Phys. Solids.

13(6) (1965) 329-350.

[5] W.H. Bowyer, M.G. Bader: J. Mater. Sci. 7(11) (1972) 1315-1321.

[6] S. Fu, B. Lauke: Compos. Sci. Technol. 56(10) (1996) 1179-1190.

[7] S. Fakirov, C. Fakirova: Polym Compos. 6(1) (1985) 41–46.

[8] R.S. Bay, C.L. Tucker III: Polym. Eng. Sci. 32(4) (1992) 240–253.

[9] F. Cosmi, A. Bernasconi: Compos. Sci. Technol. 79 (2013) 70-76.

[10] F. Cosmi: Procedia Eng. 10 (2011) 2135-2140.

[11] A. Bernasconi, F. Cosmi, D. Dreossi: Compos. Sci. Technol. 68(12) (2008) 2574-81.

[12] F. Cosmi, A. Bernasconi, N. Sodini: Compos. Sci. Technol. 71(1) (2011) 23-30.

[13] F. Cosmi: Strain 47(3) (2011) 215-221.

[14] A. Bernasconi, F. Cosmi: Procedia Eng. 10 (2011) 2129-2134.

[15] F. Cosmi, A. Bernasconi: Mater. Eng. - Mater. Inz. 17(2) (2010) 6-10.

[16] A. Bernasconi, F. Cosmi, E. Zappa: Strain 46(5) (2010) 435-445.

[17] F. Cosmi, C. Ravalico: Strain 51(3) (2015) 171-179.

[18] S.C. Cowin: Mech. Mater. 4(2) (1985) 137-147.

[19] A. Bernasconi, F. Cosmi, P.J. Hine: Compos. Sci. Technol. 72(16) (2012) 2002–2008.

[20] A. Bernasconi, E. Conrado, F. Cosmi, P. Hine: In: Proceeding of 20th International Conference on Composite Materials, 19-24 July 2015, Copenhagen (DK), available at http://www.iccm20.org/p/

[21] B.R. Whiteside, P.D. Coates, P.J. Hine, R.A. Duckett: Plast. Rubber Compos. 29(1) (2000) 38-45.

[22] L. Averous, J.C. Quantin, A. Crespy, D. Lafon: Polym. Eng. Sci. 37(2) (1997) 329-337.

[23] G.M. Luo, A.M. Sadegh, S. C. Cowin: J. Mater. Sci. 26(9) (1991) 2389-2396.

[24] T.H. Smit, E. Schneider, A. Odgaard: J. Microsc. 191(3) (1998) 249–257.

[25] R.A. Ketcham, T.M. Ryan: J. Microsc. 213(2) (2004) 158-171.

[26] ISO Standard 527-2.

[27] A. Odgaard: Bone. 2(4) (1997) 315-328.

[28] R.A. Ketcham: J. Struct. Geol. 27(7) (2005) 1217-1228.

[29] J.Schindelin, I. Arganda-Carreras, E. Frise, V. Kaynig , M. Longair, T. Pietzsch, S. Preibisch, C. Rueden, S. Saalfeld, B. Schmid, J.Y. Tinevez, D.J. White, V. Hartenstein, K. Eliceiri, P. Tomancak, A. Cardona: Nat. Methods 9(7) (2012) 676-682.

[30] S. Bolte, F.P. Cordelieres: J. Microsc. 224(3) (2006) 213-232.

[31] T.C. Lee, R.L. Kashyap, C.N. Chu: CVGIP: Graph. Model. Im. Proc. 56(6) 1994 462–478.

[32] I. Arganda-Carreras, R. Fernandez-Gonzalez, A. Munoz-Barrutia, C. Ortiz-De-Solorzano: Microsc. Res. Tech. 73(11) (2010) 1019–1029.